Journal of Pharmaceutical Analysis 8 (2018) 131–137

Contents lists available at ScienceDirect

Journal of Pharmaceutical Analysis

journal homepage: www.elsevier.com/locate/jpa
www.sciencedirect.com

Original Research Article

Eco-friendly reduced graphene oxide for the determination of mycophenolate mofetil in pharmaceutical formulations

Prashanth S. Narayan [a], Nagappa L. Teradal [a], Seetharamappa Jaldappagari [a,*], Ashis K. Satpati [b]

[a] Department of Chemistry, Karnatak University, Dharwad 580003, India
[b] Analytical Chemistry Division, Bhabha Atomic Research Centre, Trombay, Mumbai 400085, India

ARTICLE INFO

Article history:
Received 21 April 2017
Received in revised form
21 November 2017
Accepted 4 December 2017
Available online 8 December 2017

Keywords:
Mycophenolate mofetil
Electroreduced graphene oxide
Electrochemical sensor
Analytical application

ABSTRACT

Graphene oxide (GO) was synthesized and characterized by scanning electron microscopy (SEM), energy dispersive X-ray spectroscopy (EDX), atomic force microscopy (AFM), X-ray diffraction (XRD), Fourier transform-infrared spectroscopy (FT-IR) and thermogravimetric analysis (TGA). GO was then electrochemically reduced and used for electrochemical study of mycophenolate mofetil (MMF). The electrochemically reduced graphene oxide (ERGO) film on glassy carbon electrode (GCE) showed enhanced peak current for electrooxidation of MMF. MMF exhibited two irreversible oxidation peaks at 0.84 V (peak a_1) and 1.1 V (peak a_2). Effects of accumulation time, pH and scan rate were studied and various electrochemical parameters were calculated. A differential pulse voltammetric method was developed for the determination of MMF in bulk samples and pharmaceutical formulations. Linear relationship was observed between the peak current and concentration of MMF in the range of 40 nM–15 μM with a limit of detection of 11.3 nM. The proposed method is simple, sensitive and inexpensive and, hence, could be readily adopted in clinical and quality control laboratories.

1. Introduction

Graphene, a one-atom-thick sp^2 -bonded carbon sheet, has attracted the attention of scientific and technological researchers since its discovery in 2004 because of its unique properties such as high surface area, excellent electrical conductivity and high mechanical strength [1]. Compared to carbon nanotubes, graphene has the advantages of high conductivity, ease of production and function, good biocompatibility and abundance of inexpensive source material [2]. It possesses high potentials for fabricating transparent electrodes, electrochemical sensors, field effect transistors, nanocomposites, and microelectrical devices [3–6]. These properties make it a good candidate for the fabrication of inexpensive electrochemical sensors and biosensors [2,7–9].

Graphene oxide (GO) is an insulator with a large band gap and band structure that depends on stoichiometry [10,11]. It is reported that GO could be reduced by chemical reduction using reducing agents viz., hydrazine, hydroquinone, and sodium borohydride. Electrochemical methods are effective in modifying electronic states by adjusting the external power source to alter the Fermi energy level of electrode materials. In view of this, we have adopted a green method for the reduction of graphene oxide and developed an electrochemical sensor for an immunosuppressant, mycophenolate mofetil (MMF).

MMF, chemically known as 2-morpholin-4-ylethyl (E)-6-(4-hydroxy-6-methoxy-7-methyl-3-oxo-1H-2-benzofuran-5-yl)-4-methylhex-4-enoate, is a morpholinoethyl derivative of mycophenolic acid (MPA). MPA, a fermentation product of several *Penicillium* species, is a potent, noncompetitive, and reversible inhibitor of eukaryotic inosine monophosphate (IMP) dehydrogenase. MPA thus inhibits the synthesis of guanosine monophosphate. This enzyme (IMP dehydrogenase) plays an important role in the purine metabolism of lymphocytes [12,13]. It is used in the prophylaxis of graft rejection in kidney [14], heart [15], and liver transplantation [16]. It is also used following lung [17], pancreas [18] or intestine transplantation [19]. Due to its clinical advantages, several formulations of MMF are available in the market.

Recently, we have reported the electrochemical oxidation and determination of MMF in bulk sample and formulations at bare glassy carbon electrode (GCE) [20]. In order to improve the detection limits of the electrochemical method for the assay of MMF at nano molar level, we have fabricated an electrochemical sensor based on electroreduced graphene oxide (ERGO) film on GCE.

Peer review under responsibility of Xi'an Jiaotong University.
* Corresponding author.
E-mail address: jseetharam97@gmail.com (S. Jaldappagari).

https://doi.org/10.1016/j.jpha.2017.12.001

2. Experimental

2.1. Apparatus

Electrochemical investigations were carried out on a CHI-1110a Electrochemical Analyzer (CH Instruments Ltd. Co., USA, version 12.23). GCE (3 mm diameter)/ERGO-GCE and saturated calomel electrode (SCE) were used as working and reference electrodes, respectively. For reproducible results, improved detection limits and good resolution of voltammetric peaks, the working electrode was polished with 1.0, 0.3 and 0.05 μm alumina powder on a polishing cloth. Then, it was thoroughly rinsed with ultrapure water from millipore system. All the reported potentials were against SCE. Thermogram was recorded on a SDT Q 600 TG analyzer and FT-IR spectra were recorded on a Nicolet-5700 FT-IR spectrometer (Waltham, MA, USA).

A Shimadzu Maxima-7000 X-ray diffractometer with Cu K_α radiation ($\lambda = 1.5406$ Å) was used for recording powder X-ray diffraction (XRD). Scanning electron micrographs (SEM) were recorded on a Hitachi S-3400 (Japan) scanning electron microscope with an accelerating voltage of 15 kV. Composition analyses of samples were carried out on a Hitachi S-3400 SEM (Japan) coupled with a Thermo Scientific energy dispersive spectroscopic (EDS) detector at an accelerating voltage of 15 kV and a magnification of $\times 2$ K. Atomic force micrographs (AFM) were taken on a Multi-Mode Nanosurf easy scan atomic force microscope (Nanosurf, Switzerland). Commercially available AFM cantilever tips (Tap190Al-G) with a force constant of 48 N/m and resonance vibration frequency of ~ 160 kHz were used.

2.2. Reagents

Graphite powder was obtained from Sigma-Aldrich (< 20 μm). Pure MMF was a gratis sample from Dr. Reddy's Laboratories at Hyderabad, India. Tablets of MMF were obtained from commercial sources. A stock solution of MMF (0.5 mM) was prepared in a mixture of water and methanol (1:1, v/v) and stored in a refrigerator at 4 °C. In the present study, phosphate buffer solutions of pH 3.0–10.6 were used. All aqueous solutions were prepared in ultrapure water from Millipore water system (Purelab Classic Corp., USA) and the chemicals used were of analytical reagent grade. Tablet containing 500 mg of MMF (Panacea Biotec Ltd., India) was purchased commercially from the local market.

2.3. SEM/EDX

Films for SEM and EDX analysis were prepared by placing the sample suspension on a carbon film coated on a sample holder and then drying at room temperature.

2.4. Preparation of GO

GO was prepared from graphite powder (Sigma-Aldrich) by Hummers method and then dried in the oven at 120 °C [21]. The GO suspension was prepared by dispersing 10 mg of GO in 10 mL ultrapure water using ultrasonic agitation for 1 h. The yellowish brown suspension obtained was centrifuged to remove the unexfoliated GO [22]. It also resulted in the exfoliation of graphite oxide to graphene oxide. This GO suspension was used to modify the GCE.

2.5. Electrode preparation, modification and electroreduction of GO-GCE

Before modification, the GCE was carefully abraded with 1.0, 0.3 and 0.05 μm α-alumina on a smooth polishing cloth to obtain a fresh surface. It was rinsed with ultrapure water. 5 μL GO suspension was coated on GCE and then dried under an infrared lamp to obtain the GO modified electrode, denoted as GO-GCE. After modification, the electrode was rinsed with ultrapure water to remove any loosely adsorbed GO. The GO-GCE was then electroreduced in phosphate buffer of pH 6.0 by applying 25 cyclic potential sweeps between 0.6 and −1.6 V [23–25]. The modified electrode was then put in 10 mL phosphate buffer (pH 7.0) containing MMF for 120 s. After this, voltammogram (either cyclic voltammogram or differential pulse voltammogram) was recorded.

Working solutions were prepared by diluting the stock solution with 0.2 M phosphate buffer of the desired pH. All electrochemical experiments were carried out at 25 ± 1 °C. After each measurement, a new ERGO-GCE was prepared.

2.6. Analysis of tablets

Ten tablets containing MMF were ground to fine powder in a mortar. 0.2167 g of MMF was dissolved in 100 mL of water and methanol mixture (1:1, v/v) so as to obtain 0.5 mM MMF solution. Contents of the flask (0.5 mM MMF solution) were sonicated for 10 min to effect complete dissolution and for homogenization. Suitable aliquots (containing 0.05–15.0 μM MMF) of the clear liquid were diluted with the supporting electrolyte.

3. Results and discussion

3.1. Characterization

The surface morphologies of graphene derivatives such as GO and ERGO films were characterized and the corresponding SEM images are shown in Figs. 1A and B. EDX spectra of GO and ERGO are shown in Figs. 1C and D, respectively and chemical compositions of GO and ERGO are recorded in Table 1. Decreased amount of oxygen in ERGO (by about 10%) compared to that in GO indicated the reduction of oxygenated functional moieties. Further, trace amount of potassium in ERGO was observed as electrochemical reduction was carried out in phosphate buffer prepared from potassium salts. Upon electrochemical reduction of GO, the ERGO film showed a larger wrinkled and a rougher surface (Figs. 1A and B). Such rougher surface enhanced the incursion and diffusion of electrolyte ions. The electrochemical reduction of GO exposed more electrochemically active sites.

Exfoliated GO dispersion (in water) was deposited on a freshly cleaved mica sheet, dried and its surface morphology was analyzed by AFM (Fig. 2A). Height profile of the GO film is shown in Fig. 2B. The average film thickness was noticed to be approximately 7.2 nm, indicating that the film was composed of overlaying a few layers of GO sheets. Therefore, the GO film consisted of approximately 6 layers of individual GO sheets. It is also evident from 3D AFM images (Fig. 2C) that the surface morphology of GO film consisted of grooves and pores resulting in an increased microscopic area of the electrode, thereby facilitating the interlayer diffusion of analyte species.

XRD patterns of graphite and graphite oxide are illustrated in Fig. 3. A peak at ~ 26.48° was observed with pristine graphite. Disappearance of this peak and appearance of a new peak at 10.3° revealed that the graphite was successfully oxidized. Further, inter-graphene layers can be intercalated by various molecular species or ions, during which the interlayer spacing along the c-axis has changed from 3.36 to 8.55 Å. During the oxidation of graphite to graphite oxide, hydroxyl, carbonyl, epoxy and peroxy groups could be formed on the edges of basal planes of the graphite network [26]. Further, carbon hydrolyzation could occur and

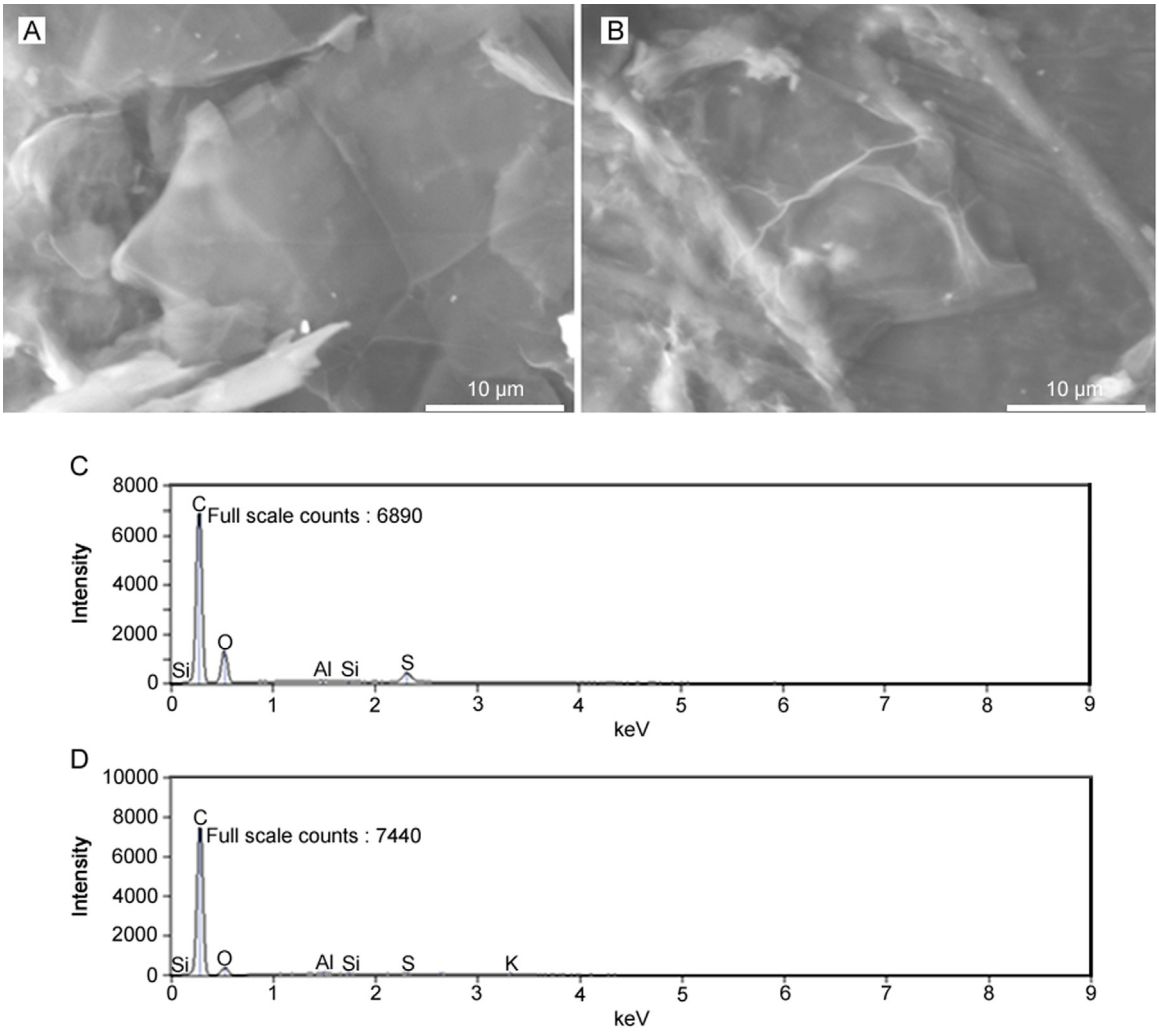

Fig. 1. Scanning electron micrographic images of (A) GO and (B) ERGO, and EDX spectra of (C) GO and (D) ERGO.

Table 1
Chemical composition (%) of GO and ERGO obtained from energy dispersive X-ray spectroscopic (EDX) analysis.

Element	Carbon	Oxygen	Aluminium	Silicon	Sulphur	Potassium	Total
GO	77.69	17.10	0.39	0.30	4.52	–	100
ERGO	91.51	5.90	0.26	0.15	0.78	1.40	100

the sp^2 bonds could be changed to sp^3 bonds. At the same time, H_2O, NO_3^- or SO_4^{2-} ions could insert themselves into the graphene layers and increase the interlayer spacing [26–28].

To determine the degree of oxidation and to determine the percentage of oxygen containing groups in graphite oxide, the synthesized graphite oxide was characterized by FT-IR spectroscopy and thermogravimetric analysis (Figs. S1 and S2). Thermogram was recorded at a heating rate of 10 °C/min under nitrogen atmosphere from ambient temperature to 1000 °C. The weight loss at initial stages of heating corresponded to the liberation of small amounts of water. Significant amount of weight loss (around 20%) accompanied by a DTA peak was noticed at ~ 200 °C, indicating the decomposition of oxygen containing groups in GO. Another weight loss noticed at ~ 700 °C was assigned to the burning of carbon backbone [29,30]. The relative amount of functional groups was found to be 32%.

FT-IR spectrum of GO exhibited bands at 1713 and 1100 cm^{-1} due to the presence of a large number of carboxyl and epoxide groups, respectively [30].

3.2. Electrochemical reduction of GO-GCE

The electrochemical reduction of GO-GCE was carried out in 0.2 M phosphate buffer of pH 7.0 by cycling the potential between 0.6 and −1.6 V for 25 cycles. The first cycle showed a broad reduction peak at a potential of −1.4 V due to the reduction of oxygen containing surface groups [25,31]. With successive cycles, the reduction peak diminished considerably and vanished after a few cycles. This showed that the electrochemical reduction of oxygen containing groups in graphene oxide was complete. Effective electrode area of the modified electrode was determined using 1 mM K_3 [Fe $(CN)_6$] as a redox probe and found to be 6 times more than that of bare GCE.

3.3. Electrochemical oxidation of MMF at ERGO-GCE

Cyclic voltammograms of 5 μM MMF in phosphate buffer of pH 7.0 at bare GCE and ERGO-GCE with a scan rate of 100 mV/s were recorded. It was observed that MMF exhibited two irreversible

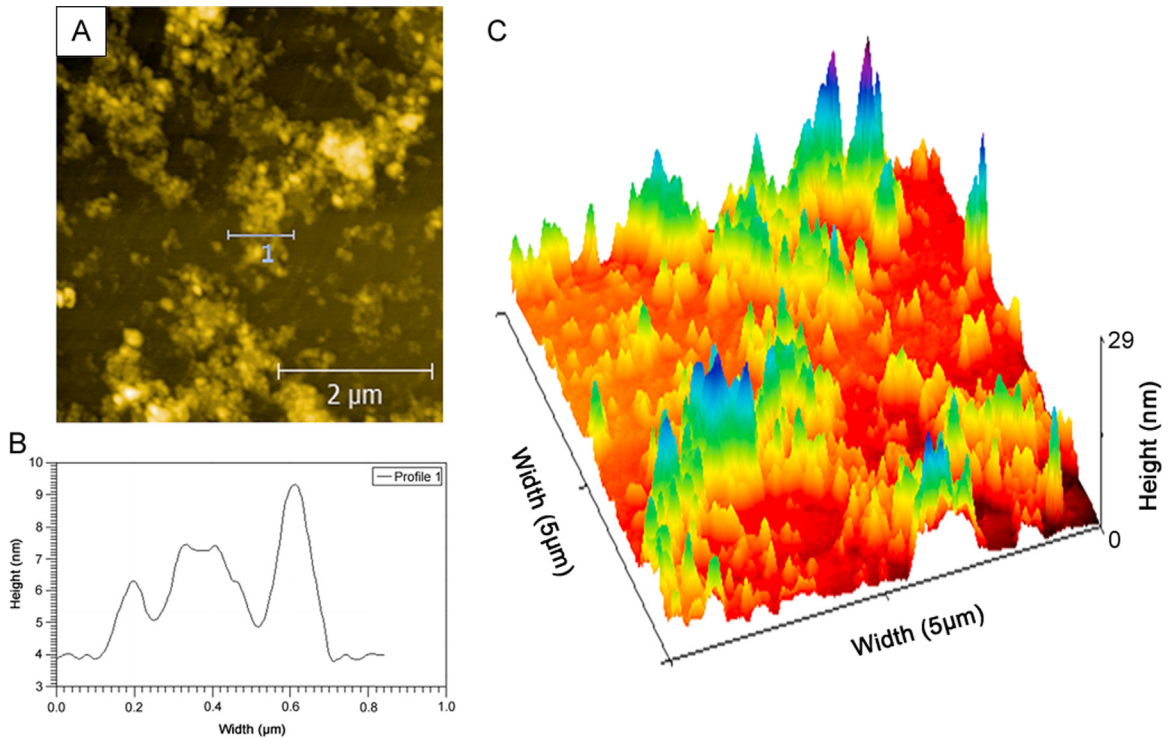

Fig. 2. (A) AFM images of GO, (B) Height profile of GO and (C) 3D AFM image of GO film coated on a freshly cleaved mica sheet.

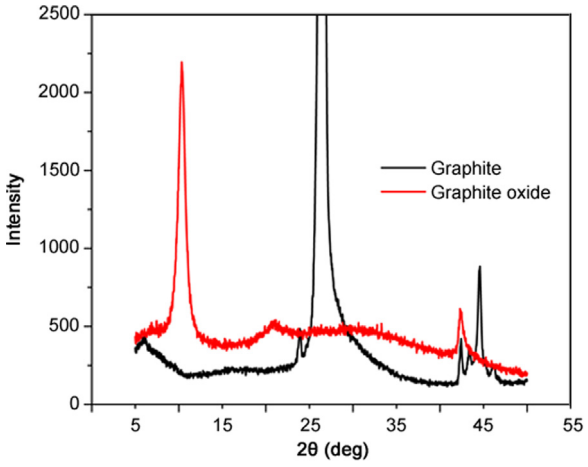

Fig. 3. X-ray diffraction patterns of graphite oxide (red) and pristine graphite (black).

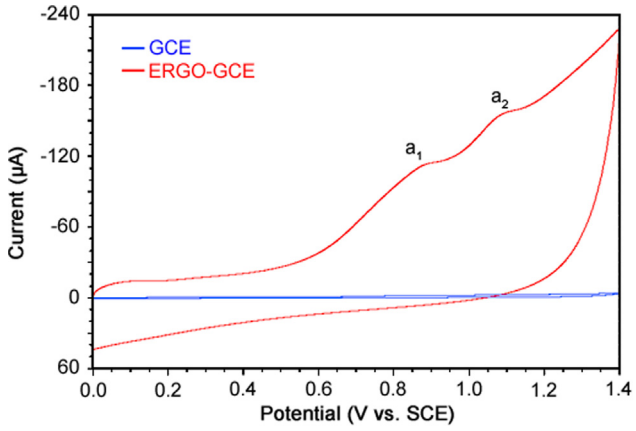

Fig. 4. Cyclic voltammograms of 5 µM MMF in phosphate buffer of pH 7.0 at a scan rate of 100 mV/s at bare and ERGO-GCE.

oxidation peaks designated as peak a_1 and a_2 respectively (Fig. 4). A large background current was observed at ERGO-GCE compared to that at bare GCE due to larger surface area of ERGO film on GCE [32]. The oxidation signal of MMF was enhanced to a greater extent at ERGO-GCE in comparison with that at bare GCE, signifying that the ERGO enhanced the electro-oxidation of MMF. It might be correlated to exceptional properties of graphene such as high electrical conductivity and specific surface area, and good adsorption characteristics.

To study the adsorption characteristics of MMF or its oxidation products, multi-sweep cyclic voltammograms of 5 µM MMF were recorded in phosphate buffer of pH 7.0 at a sweep rate of 100 mV/s. Peak currents were found to decrease with consecutive voltammetric sweeps, signifying that the oxidation products of MMF were adsorbed on ERGO-GCE surface and caused fouling of the electrode. This could be attributed to poor solubility of the oxidized product of MMF that was accumulated on the electrode surface during the electrode process. This reduced the effective reaction sites on the modified electrode surface [33].

3.4. Effect of accumulation time

Accumulation time plays an important role in electrochemical oxidation of molecules. So, the effect of accumulation time on electrochemical oxidation of MMF was investigated by cyclic voltammetry. For this, cyclic voltammograms of MMF were recorded in phosphate buffer of pH 7.0 by varying accumulation time from 0 to 240 s. As the accumulation time increased from 0 to 120 s, peak currents increased gradually owing to the increased surface area of MMF on ERGO. After 120 s, the peak currents did not show any substantial change, indicating the surface saturation by the analyte. Therefore, 120 s was chosen as optimum accumulation time for further studies.

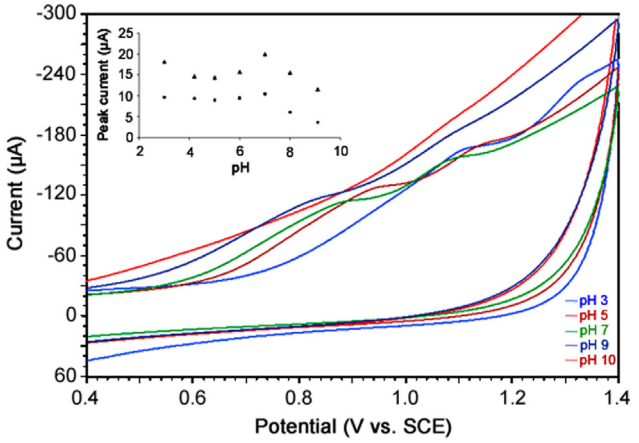

Fig. 5. Cyclic voltammograms of 5 μM MMF in phosphate buffer of different pH at a scan rate of 100 mV/s. Inset: Plots of peak currents versus pH for oxidation peaks a_1(▲) and a_2 (■).

3.5. Effect of pH on the electrochemical oxidation of MMF

The effect of electrolyte pH on electrochemical oxidation of MMF was investigated by cyclic voltammetry in phosphate buffer of pH 3.0–10.0 (Fig. 5). The peak currents of both oxidation peaks, a_1 and a_2, showed variation and maximum peak current was noticed at pH 7.0 (inset of Fig. 5). Hence, phosphate buffer of pH 7.0 was selected as supporting electrolyte for further investigations.

Peak potentials of peak a_1 and a_2 exhibited negative shift with increase in pH of the solution (3.0–9.0), indicating the involvement of protons in the electrochemical oxidation of MMF. Further, the plots of E_p versus pH revealed the linear relationship in the pH range of 3.0–8.0 with slope values of 64 mV/pH and 55 mV/pH for oxidation peaks, a_1 and a_2, respectively, indicating that an equal number of electrons and protons were involved in the electrode process. The corresponding regression equations are shown below:

$$E_{pa}(V) = -0.064\ pH + 1.3 \quad (\text{for peak } a_1)$$

$$E_{pa}(V) = -0.055\ pH + 1.5 \quad (\text{for peak } a_2)$$

3.6. Effect of scan rate

Considerable information regarding the type of electrode process can be obtained from the study of effect of scan rate on electrochemical oxidation. So, the effect of scan rate on peak currents and peak potentials of both oxidation peaks a_1 and a_2 of MMF (5 μM) was studied in phosphate buffer of pH 7.0 and the results are shown in Fig. 6. The peak currents (I_p) increased linearly with scan rate (ν) (inset of Fig. 6) in the range of 10–300 mV/s, indicating the adsorption controlled electrode process for both peaks a_1 and a_2 [34], and the corresponding regression equations are indicated below:

$$I_p(A) = 1.20 \times 10^{-4}\ \nu + 2.81 \times 10^{-6} (r = 0.992) \quad (\text{for peak } a_1)$$

$$I_p(A) = 7.61 \times 10^{-5}\ \nu + 2.09 \times 10^{-7} (r = 0.991) \quad (\text{for peak } a_2)$$

Further, to confirm the electrode process, we plotted the values of log I_p versus log ν. The slope value of 0.75 for peak a_1 indicated the contribution from diffusion to the electrode process. Hence, it was proposed that the electrode reaction for peak a_1 of MMF at ERGO-GCE was a "mixed" diffusion–adsorption controlled process [35]. However, the slope value of 1.01 for peak a_2 confirmed the adsorption controlled electrode process [36].

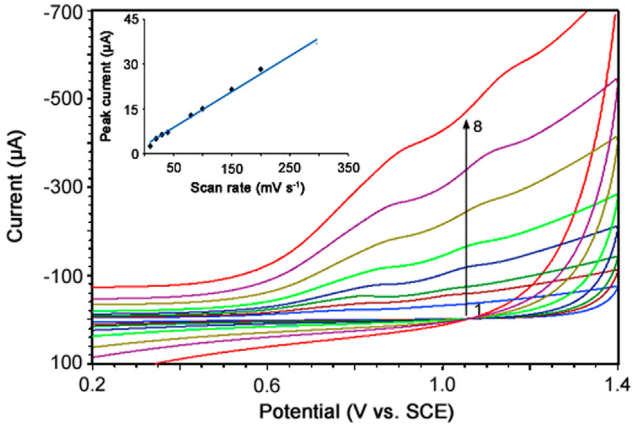

Fig. 6. Effect of scan rate on cyclic voltammograms of 5 μM MMF at 10 (1), 30 (2), 40 (3), 80 (4), 100 (5), 150 (6), 200 (7) and 300 mV/s (8). Inset: Plot of peak current versus scan rate for electrooxidation of 5 μM MMF in phosphate buffer of pH 7.0.

The corresponding regression equations are given below:

$$\log I_{pa} = 0.75\ \log \nu - 4.06 \quad (r = 0.995) \quad (\text{for peak } a_1)$$

$$\log I_{pa} = 1.01\ \log \nu - 4.11 \quad (r = 0.978) \quad (\text{for peak } a_2)$$

3.7. Analytical features

3.7.1. Construction of calibration plot

We have developed a differential pulse voltammetric (DPV) method for the determination of MMF in bulk sample because the peaks were sharper and better defined at lower concentrations of MMF with a lower background current, resulting in better resolution between the peaks compared to those obtained by CV. The following parameters were maintained for the determination of MMF by DPV: sweep rate, 20 mV/s; pulse amplitude, 50 mV; pulse width, 30 ms; and pulse period, 500 ms. The differential pulse voltammograms of increased concentrations of bulk MMF samples were recorded in phosphate buffer of pH 7.0 (Fig. 7). Under optimized conditions, the peak current was found to vary linearly with increasing concentrations of MMF in the range of 40 nM–15 μM (Inset of Fig. 7). Deviation from linearity was observed at higher concentrations of MMF owing to the adsorption of oxidation products of MMF on the electrode surface.

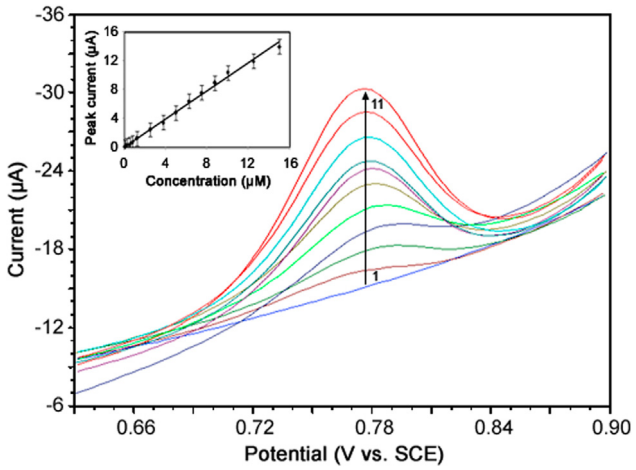

Fig. 7. Differential pulse voltammograms of MMF in phosphate buffer of pH 7.0 for (1) 0.04, (2) 1.25, (3) 2.5, (4) 3.75, (5) 5.00, (6) 6.25, (7) 7.50, (8) 8.75, (9) 10.00, (10) 12.50 and (11) 15.00 μM MMF. Inset: Plot of peak current versus concentration of MMF in phosphate buffer of pH 7.0.

Table 2
Results of analysis of MMF in tablets.

Tablet	Labeled claim (mg)	Amount found (mg)	Recovery[b] (%)	t-value[*]	F-value[*]
Mycept[a]	500.0	496.7	99.34	0.14	4.39
Mycept[#]	500.0	490.0	98.00	–	–

[*] @ 95% confidence level.
[a] Mycept contains 500 mg MMF and it is marketed by Panacea Biotec.
[b] Average of 5 determinations.
[#] Reported voltammetric method using GCE [20].

Validation of the proposed DPV method for quantification of MMF was examined by calculating the values of limit of detection (LOD) and limit of quantification (LOQ) using the following equations [37]:

$$LOD = 3\ s/m;\ \ LOQ = 10\ s/m$$

where s is the standard deviation of the lowest concentration value within the linear range and m is the slope of the calibration plot. Low values of LOD (11.3 nM) and LOQ (37.5 nM) highlighted the sensitivity of the proposed method. Characteristics of the calibration plot are shown in Table S1. The values of RSD for intra-day and inter-day assay were found to be 2.46% and 2.13%, respectively, indicating good reproducibility of results.

Recently, multiwalled carbon nanotube (MWCNT) modified GCE was applied for the determination of MMF and mycophenolic acid [38]. The proposed/developed DPV method has lower value of LOD (11.3 nM) compared to that of the reported (900 nM) electrochemical method [38]. The major advantage of graphene modified electrode is the incorporation of thin layer diffusion channel in addition to the semi-infinite planar diffusion. This additional channel of mass transport has enhanced the amount of mass transfer, which eventually improved the LOD of the method by many folds. The other important advantage of graphene is the ease of renewability compared to MWCNTs due to its thinner layer (helpful in bringing back the analyte after oxidation). As a result, the LOD of the proposed method was achieved at a nano molar level.

3.7.2. Stability and reproducibility of ERGO-GCE

The ERGO film sensor was used for solitary measurement and the reproducibility of the proposed sensor (ERGO-GCE) was examined by parallel determinations of 5 μM MMF by DPV. The value of RSD was found to be 3.2% for 5 GO film sensors, thereby revealing good reproducibility. The ERGO-GCE exhibited 95% of its original current response when stored in a refrigerator (at 4 °C) for 3 weeks, indicating that the electrode had long-term stability.

3.7.3. Interference studies

In order to demonstrate practical application of the proposed method, the effect of some common excipients generally present in pharmaceutical formulations was examined in the determination of MMF. The results showed that a 75-fold excess of glucose, lactose, sucrose, talc, gum acacia, cellulose and starch had a negligible influence on oxidation signals of MMF with peak current deviations below 5.0%. These results clearly supported the reasonable selectivity of the proposed method.

3.7.4. Analysis of pharmaceutical formulations and comparison with the reported method

In order to examine applicability of the proposed method, the sensor was used to determine MMF in commercially available tablets under optimized conditions. The results of assay of tablets containing MMF are summarized in Table 2. Accuracy of the proposed method was evaluated by performing recovery test after spiking known amounts of the samples. Higher recovery (more than 99.5%) and low bias values (0.5%) confirmed the accuracy of the proposed method.

The results were compared statistically by Student t-test and by the variance ratio F-test with those obtained by the reported method [20]. The calculated Student t-value at 95% confidence level did not exceed the tabulated value, thereby revealing that there was no significant difference in accuracy between the proposed and reported methods. Further, it was also observed that the variance ratio F-value calculated for $p = 0.05$ did not exceed the tabulated value, indicating that there was no significant difference in precision of the proposed and reported methods.

4. Conclusions

In the present work, we have used an eco-friendly electrochemical method for the reduction of GO to ERGO. AFM, SEM, EDX, XRD, FT-IR and TGA techniques were employed to characterize the synthesized GO. The fabricated electrode showed good sensing performance for MMF. Wide linearity, lower LOD value and excellent reproducibility highlighted ERGO-GCE as a promising sensor for MMF.

Conflicts of interest

The authors declare that there are no conflicts of interest.

Acknowledgments

We are grateful to the Board of Research in Nuclear Sciences, Mumbai, for financial assistance (No.2012/37C/8/BRNS/637 dated 28-05-2012). Thanks also go to the authorities of the Karnatak University, Dharwad, for providing the necessary facilities.

Appendix A. Supplementary material

Supplementary data associated with this article can be found in the online version at doi:10.1016/j.jpha.2017.12.001.

References

[1] K.S. Novoselov, A.K. Geim, S.V. Morozov, et al., Electric field effect in atomically thin carbon films, Science 306 (2004) 666–669.
[2] M. Pumera, A. Ambrosi, A. Bonanni, et al., Graphene for electrochemical sensing and biosensing, Trends Anal. Chem. 29 (2010) 954–965.
[3] P. Blake, P.D. Brimicombe, R.R. Nair, et al., Graphene-based liquid crystal device, Nano Lett. 8 (2008) 1704–1708.
[4] H.A. Becerril, J. Mao, Z. Liu, et al., Evaluation of solution-processed reduced graphene oxide films as transparent conductors, ACS Nano 2 (2008) 463–470.
[5] D. Li, M.B. Muller, S. Gilje, et al., Processable aqueous dispersions of graphene nanosheets, Nat. Nanotechnol. 3 (2008) 101–105.
[6] I. Meric, M.Y. Han, A.F. Young, et al., Current saturation in zero-bandgap, top-gated graphene field-effect transistors, Nat. Nanotechnol. 3 (2008) 654–659.
[7] Y. Shao, J. Wang, H. Wu, et al., Graphene based electrochemical sensors and biosensors: a review, Electroanalysis 22 (2010) 1027–1036.
[8] B.J. Sanghavi, W. Varhue, J.L. Chávez, et al., Electrokinetic preconcentration and detection of neuropeptides at patterned graphene-modified electrodes in a nanochannel, Anal. Chem. 86 (2014) 4120–4125.
[9] B.J. Sanghavi, S. Sitaula, M.H. Griep, et al., Real-time electrochemical monitoring of adenosine triphosphate in the picomolar to micromolar range using graphene-modified electrodes, Anal. Chem. 85 (2013) 8158–8165.
[10] J. Yan, L. Xian, M.Y. Chou, Structural and electronic properties of oxidized graphene, Phys. Rev. Lett. 103 (2009) 086802.
[11] D.W. Boukhvalov, M.I. Katsnelson, Modeling of graphite oxide, J. Am. Chem. Soc. 130 (2008) 10697–10701.
[12] P. Leyssen, N. Charlier, J. Paeshuyse, et al., Prospects for antiviral therapy, Adv. Virus Res. 61 (2003) 511–553.
[13] B. Tönshoff, A. Melk, Book Chapter59, Immunosuppression in pediatric kidney transplantation, Comprehensive Pediatric Nephrology, Springer, Heidelberg, 2008: 905–929.

[14] D.C. Brennan, M.J. Koch, Pierratos A: daily nocturnal hemodialysis - a paradigm shift worthy of disrupting current dialysis practice, Nat. Clin. Pract. Nephr. 3 (2007) 602–603.
[15] P. Mathieu, M. Carrier, M. White, et al., Effect of mycophenolate mofetil in heart transplantation, Can. J. Surg. 43 (2000) 202–206.
[16] T.M. Manzia, N.D.L. Carino, G. Orlando, et al., Use of mycophenolate mofetil in liver transplantation: a literature review, Transplant. Proc. 37 (2005) 2616–2617.
[17] A. Zuckermann, T. Birsan, S. Thaghavi, et al., Mycophenolate mofetil in lung transplantation, Transplant. Proc. 30 (1998) 1514–1516.
[18] R.W. Gruessner, D.E. Sutherland, M.B. Drangstveit, et al., Mycophenolate mofetil in pancreas transplantation, Transplantation 66 (1998) 318–323.
[19] M. Cantarovich, N.W. Brown, M.H.H. Ensom, et al., Mycophenolate monitoring in liver, thoracic, pancreas, and small bowel transplantation: a consensus report, Transplant. Rev. 25 (2011) 65–77.
[20] S.N. Prashanth, K.C. Ramesh, J. Seetharamappa, Electrochemical oxidation of an immunosuppressant, mycophenolate mofetil, and its assay in pharmaceutical formulations, Int. J. Electrochem. 2011 (2011) 1–7.
[21] H. Yu, B. Zhang, C. Bulin, et al., High-efficient Synthesis of graphene oxide based on improved Hummers method, Sci. Rep. 6 (2016) 36143.
[22] S. Park, R.S. Ruoff, Chemical methods for the production of graphenes, Nat. Nanotechnol. 4 (2009) 217–224.
[23] J. Wang, S. Yang, D. Guo, et al., Comparative studies on electrochemical activity of graphene nanosheets and carbon nanotubes, Electrochem. Commun. 11 (2009) 1892–1895.
[24] N.L. Teradal, P.S. Narayan, A.K. Satpati, et al., Fabrication of electrochemical sensor based on green reduction of graphene oxide for an antimigraine drug, rizatriptan benzoate, Sens. Actuators B 196 (2014) 596–603.
[25] T. Chen, Z. Sheng, K. Wang, et al., Determination of explosives using electrochemically reduced graphene, Chem. Asian J. 6 (2011) 1210–1216.
[26] C. Hontoria-Lucas, A.J. López-Peinado, J. de D. López-González, et al., Study of oxygen-containing groups in a series of graphite oxides: physical and chemical characterization, Carbon 33 (1995) 1585–1592.
[27] H.Y. He, T. Riedl, A. Lerf, et al., Solid-state NMR studies of the structure of graphite oxide, J. Phys. Chem. 100 (1996) 19954–19958.
[28] H.Y. He, J. Klinowski, M. Forster, et al., A new structural model for graphite oxide, Chem. Phys. Lett. 287 (1998) 53–56.
[29] G. Wang, J. Yang, J. Park, et al., Facile synthesis and characterization of graphene nanosheets, J. Phys. Chem. C 112 (2008) 8192–8195.
[30] M. Jin, H. Jeong, T. Kim, et al., Synthesis and systematic characterization of functionalized graphene sheets generated by thermal exfoliation at low temperature, J. Phys. D: Appl. Phys. 43 (2010) 275402.
[31] H.L. Guo, X.F. Wang, Q.Y. Qian, et al., A green approach to the synthesis of graphene nanosheets, ACS Nano 3 (2009) 2653–2659.
[32] S.F. Wang, F.R. Xie, F. Hu, Carbon-coated nickel magnetic nanoparticles modified electrodes as a sensor for determination of acetaminophen, Sens. Actuators B 123 (2007) 495–500.
[33] A. Veiga, A. Dordio, A.J.P. Carvalho, et al., Ultra-sensitive voltammetric sensor for trace analysis of carbamazepine, Anal. Chim. Acta 674 (2010) 182–189.
[34] Y. Guo, S. Guo, J. Li, et al., Cyclodextrin–graphene hybrid nanosheets as enhanced sensing platform for ultrasensitive determination of carbendazim, Talanta 84 (2011) 60–64.
[35] S.N. Prashanth, N.L. Teradal, J. Seetharamappa, et al., Fabrification of electroreduced graphene oxide–bentonite sodium composite modified electrode and its sensing application for linezolid, Electrochim. Acta 133 (2014) 49–56.
[36] P.S. Narayan, N.L. Teradal, S.S. Kalanur, et al., Fabrication of an electrochemical sensor based on multiwalled carbon nanotubes for almotriptan, Electroanalysis 25 (2013) 2684–2690.
[37] S. Skrzypek, W. Ciesielski, A. Sokolowski, et al., Square wave adsorptive stripping voltammetric determination of famotidine in urine, Talanta 66 (2005) 1146–1151.
[38] T. Madrakian, M. Soleimani, A. Afkhami, Simultaneous determination of mycophenolate mofetil and its active metabolite, mycophenolic acid, by differential pulse voltammetry using multi-walled carbon nanotubes modified glassy carbon electrode, Mater. Sci. Eng. C 42 (2014) 38–45.